Current Applied Physics 13 (2013) 2005–2009

Contents lists available at ScienceDirect

Current Applied Physics

journal homepage: www.elsevier.com/locate/cap

Origin of the ferromagnetism in ZnCoO from chemical reaction of Co_3O_4

Seunghun Lee [a], Bum-Su Kim [a], Yong Chan Cho [b], Jong-Moon Shin [c], Seung-Wan Seo [d], Chae Ryong Cho [e], Ichiro Takeuchi [c], Se-Young Jeong [a, *]

[a] Department of Cogno-Mechatronics Engineering, Pusan National University, Miryang 627-706, Republic of Korea
[b] Crystal Bank Research Institute, Pusan National University, Miryang 627-706, Republic of Korea
[c] Materials and Science Engineering, University of Maryland, College Park, MD 20742, United States
[d] School of Environmental Science and Engineering, POSTECH, Pohang 790-784, Republic of Korea
[e] Department of Nano Fusion Technology, Pusan National University, Miryang 627-706, Republic of Korea

ARTICLE INFO

Article history:
Received 9 July 2013
Received in revised form
19 August 2013
Accepted 20 August 2013
Available online 10 September 2013

Keywords:
ZnCoO
Hydrogen
M–T curve
Co nano cluster

ABSTRACT

We investigated conversion of Co_3O_4 to Co nanoclusters through hydrogen reduction. Quantitative analysis is performed on the conversion of Co_3O_4 to Co metal as a function of hydrogen-injection conditions. Our results reveal that Co_3O_4 must be completely eliminated to avoid formation of the metal phase in ZnCoO. We also propose a new M–T curve based method for detecting nano-sized Co clusters which are below the detection limit of diffraction techniques. It is also found that the Co phase can be transformed back to the Co_3O_4 phase through oxygen annealing and that, as a result, the ferromagnetism can be eliminated. These findings are discussed in the context of the origin of ferromagnetism in ZnCoO.

1. Introduction

Since room-temperature ferromagnetism (RTFM) in transition metal (TM)-doped wide-band gap semiconductors has been theoretically predicted, TM-doped semiconducting oxides, such as ZnO and TiO_2, have attracted wide interest [1,2]. Several studies have been attempted to realize RTFM in semiconducting oxides; however, realization of RTFM remains to be a challenge. Even though ferromagnetism has been predicted in many systems, experimental studies have produced inconsistent results and the origin of ferromagnetism still remains unclear [3–9]. There have been some reports on successful induction of ferromagnetism in ZnCoO through hydrogen doping [10–17]. Hydrogen treatment has been widely used to introduce hydrogen impurity or crystalline defects in oxide semiconductor for studying on their effects on magnetic properties of ZnCoO [18–21]. However, it may promote chemical reduction of oxygen bonding. S. Deka et al. reported that hydrogenation process causes chemical reduction of Co–O bonding and creates Co metallic phase which is an extrinsic ferromagnetic source [22]. For this reason, it is necessary to demonstrate absence of ferromagnetic secondary phases to clearly identify the controversial magnetic characteristics of ZnCoO [10–12]. However, as will be shown later, it is difficult to detect nano-scale Co metallic clusters even with high-resolution diffraction experiments.

Co in oxide semiconductors can chemically form various Co-related secondary phases, such as CoO, Co_2O_3, and Co_3O_4. Formation of these phases strongly depends on the sample fabrication conditions (e.g. temperature or Co doping concentrations) [10,23]. Among those phases, CoO and Co_3O_4 were not considered to be secondary phases of RTFM ZnCoO because these phases have antiferromagnetism instead of ferromagnetism [12,24,25]. However, it is noted that Co oxides can be easily converted into a Co metal phase in the post treatment process through chemical reduction [12,26,27]. Therefore, one has to consider such possibility in the study of RTFM in ZnCoO.

The purpose of the work in this letter is to investigate possibility of ferromagnetism in ZnCoO originating from Co_3O_4. We report on study of structural and magnetic changes in Co_3O_4 powder upon the hydrogen treatment. Our results suggest that temperature-dependent magnetization measurement can be employed in quantitative detection of nano-sized Co metal clusters in small quantities which are currently undetectable by structural

* Corresponding author.
E-mail address: syjeong@pusan.ac.kr (S.-Y. Jeong).

1567-1739/$ – see front matter © 2013 Elsevier B.V. All rights reserved.
http://dx.doi.org/10.1016/j.cap.2013.08.014

diffraction measurements. Given these findings, we assert that Co_3O_4 phase should be carefully examined and removed prior to the post treatments to prevent ferromagnetic contribution from Co metal cluster in ZnCoO.

2. Experimental details

Co_3O_4 powder was fabricated by the sol–gel method, which is conventionally used for fabricating ZnCoO, as described in our previous reports [10–13]. Radio frequency (rf) plasma treatment was used for the hydrogen injection process. Co_3O_4 powders were exposed for 10 min per treatment to hydrogen plasma with varying rf-power (20 ~ 80 W), using Ar:H_2 (9:1 vol%) mixed gas. X-ray diffraction (XRD) was performed to examine change in crystallinity as well as formation of secondary phases. Magnetization characteristic was determined as a function of the applied magnetic field (M–H) and temperature (M–T), using a vibrating sample magnetometer installed in the physical-property measurement system (VSM: model 6000, Quantum Design, Inc.).

3. Result and discussion

Fig. 1 shows the M–H and M–T curves of Co_3O_4 powder samples, heat-treated at two different temperatures (300 °C and 500 °C). The XRD patterns of both Co_3O_4 samples correspond to that of pure Co_3O_4 phase; no other Co-related secondary phases were observed within the detection limit of the measurement, irrespective of the heat-treatment temperature (not shown here). The peak widths of both Co_3O_4 powder samples were almost the same, which indicates similar particle sizes in the samples. M–H curves of the Co_3O_4 sample heat-treated at 300 °C show a ferromagnetic hysteresis loop both at 300 K and 10 K (Fig. 1(a)). Its M–T curve (Fig. 1(b)) shows a weak sign of an inflection temperature. The temperature is close to the Neel temperature of Co_3O_4 ($T_N = 40$ K [24]), but the magnetic transition was not clear. It was assumed to be related to coexistence of some ferromagnetic phases and antiferromagnetic Co_3O_4. However, M–H curves of Co_3O_4 heat-treated at 500 °C exhibits a linear behavior both at 300 K and 10 K (Fig. 1(c)). Besides, its M–T curve clearly shows a Neel temperature at 40 K (Fig. 1(d)), which is the intrinsic behavior of Co_3O_4 [24]. The magnetization of the sample heat-treated at 500 °C decreases to about one sixth of that of the sample treated at 300 °C. Note that all XRD patterns of samples treated at 300 °C correspond to single-phase Co_3O_4; thus, it may be concluded that the ferromagnetism is caused by Co organic compounds, nano size effect [28,29] or ferromagnetic precipitates beyond the XRD detection limit which can be eliminated by high temperature heat treatment.

We examined changes in structural and magnetic properties of Co_3O_4 as a function of hydrogen injection with various degrees of rf power and number of sample exposure to the plasma. Co_3O_4 powder fabricated at 500 °C was used for this study, which exhibits the typical characteristics of Co_3O_4 with a Neel temperature. Fig. 2 shows XRD patterns from Co_3O_4 powders for various hydrogen-treatment conditions. The numbers on the left and right sides of the hyphen (-) in each label denote the rf-power and number of hydrogen plasma exposure, respectively (e.g. H20-4 means Co_3O_4 powder treated at 20 W for 4 times.). The sample H40-1 showed only the Co_3O_4 single phase within the XRD detection limit. The samples hydrogenated at <40 W are not presented here because they show results very similar to that of single phase Co_3O_4. However, additional peaks comparable to the background noise level arise in the XRD pattern for H60-1. These correspond to CoO and hexagonal Co metal phases (marked by the green asterisks in the diffraction patterns for each sample), and are attributed to the reduction of Co_3O_4 by hydrogen treatment [12]. Additional diffraction patterns are more clear with the rf-power is increased as shown in XRD pattern for H80-1. However, even in the logarithm scale plot of the intensity for clear observation of the background level, it is not easy to clearly identify them. It reflects the difficulty in the detection of secondary phases in oxide semiconductors due to the fact that their quantity and size are smaller than the detection limit of diffraction techniques.

We instead try to see the changes in magnetic properties as a function of hydrogen injection. To do it, the M–H and M–T curves were obtained for various hydrogen plasma conditions as shown in Fig. 3. Fig. 3(a) shows M–H curves for H20-1 and H20-4 samples.

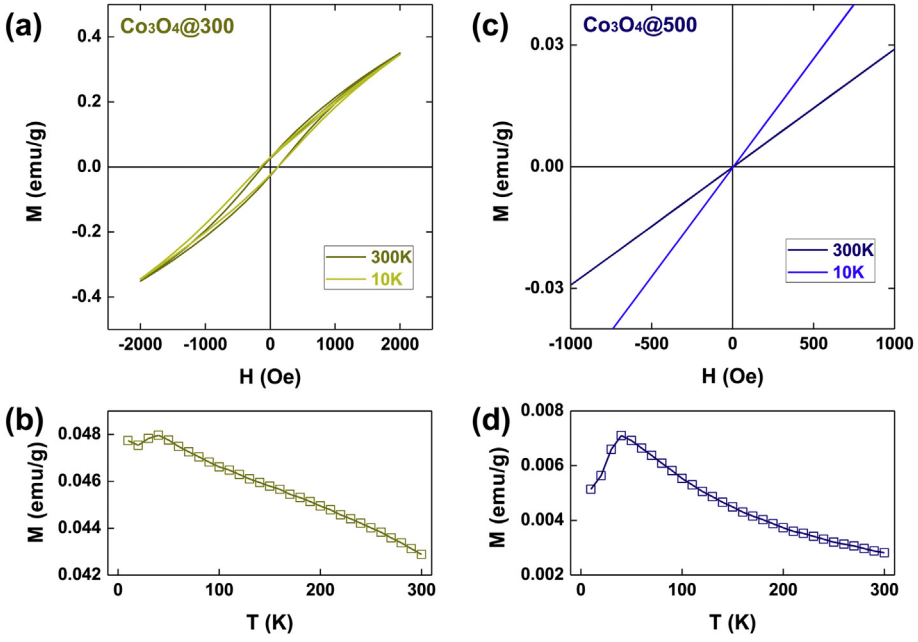

Fig. 1. (a) Magnetization–applied magnetic field (M–H) characteristics and (b) magnetization–temperature (M–T) characteristics of Co_3O_4 after thermal treatment at 300 °C. (c) M–H and (d) M–T characteristics of Co_3O_4 powder after thermal treatment at 500 °C.

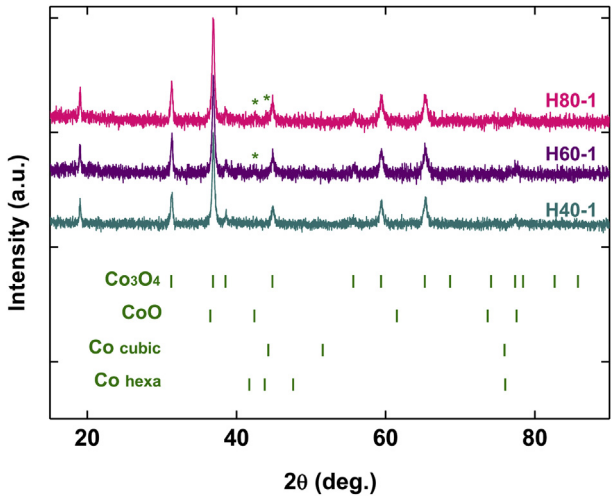

Fig. 2. X-ray diffraction (XRD) patterns of hydrogenated Co_3O_4 powders of H40-1, H60-1, and H80-1 treated under 40 W, 60 W, and 80 W of rf power, respectively, where 1 stands for the number of plasma treatments. The green asterisks represent the additional peaks not corresponding to the Co_3O_4 phase. (For interpretation of the references to colour in this figure legend, the reader is referred to the web version of this article.)

The curves obtained at 300 K exhibit a weak ferromagnetic hysteresis whereas 10 K data were much closer to that of a paramagnetic material (inset of Fig. 3(a)). We may attribute the weak ferromagnetism to creation of Co metal phase through chemical reduction. However, it is rather anomalous to see that the sample becomes paramagnetic at a low temperature even though it is far below the Curie temperature (~1388 K). Therefore, we assumed that the abnormality is related to formation of nano-sized Co metallic phase. Clear Neel transition temperature observed in H20-1 and H20-4 (Fig. 3(b)) reflects the fact that the magnetic contribution of Co_3O_4 is still dominant. Interestingly, in the M–T curves, the magnetizations of H20-1 and H20-4 increase with increasing temperature above 250 K. We will discuss this phenomenon in detail, later. It appears that the weak ferromagnetic behavior from the other phase is seen only above this temperature: when magnetism from Co_3O_4 becomes very weak. We also note that the magnetization increases with increasing number of hydrogen treatments. The ferromagnetic behavior was more pronounced for H40-1 (Fig. 3(c)) even though its XRD pattern showed no clear secondary phase. This was also the case for H60-1 in which the secondary phase was detected (Fig. 2), having 10 times larger magnetization than that of H40-1. The M–T curves for H40-1 and H60-1 no longer exhibit a Neel transition (Fig. 3(d)). These observations indicate that the ferromagnetism from Co phase become much more dominant than the weak antiferromagnetism of Co_3O_4 as the number of treatment increases. The magnetization decreases with increasing temperature overall, but weak and broad anomalies near 150 K and 250 K were observed for H40-1 and H60-1, respectively, which is assumed to be due to the existence of phases other than Co_3O_4 as well as magnetic interactions between these phases.

It is worthwhile to note that above 250 K for H20-1 and H20-4, the magnetization increases with increasing temperature while the antiferromagnetic material exhibits a negative magnetization slope above the Neel temperature. The abnormal magnetic behaviors observed in H20-1 and H20-4 (the linear behavior in M–H curves at 10 K and the small hysteresis loop at 300 K as well as positive slope in M–T curves) support the conjecture of the inclusion of nano-sized Co metallic phases. It has been reported that the absence of magnetic anisotropy is related to the abnormal magnetic behavior of the Co nano cluster [30,31]. Considering the fact that no additional phase was detected with XRD in H20 series, the quantity and size of ferromagnetic precipitate have to be very small, a view that

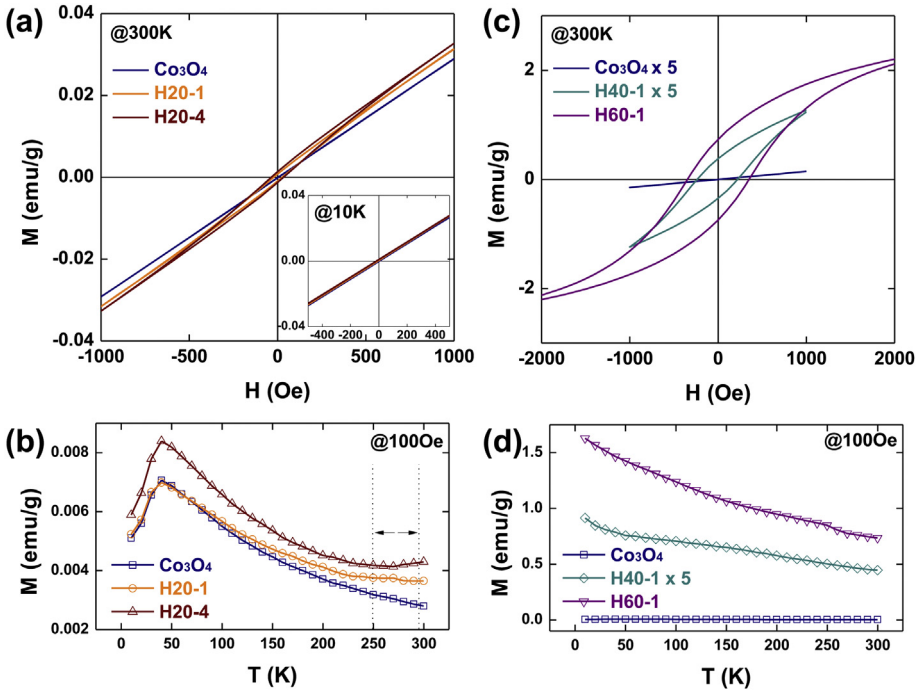

Fig. 3. (a) M–H curves of H20-1 and H20-4, which represent the hydrogen plasma-treated Co_3O_4 under rf power of 20 W once and four times, respectively, and (b) their M–T curves. (c) M–H curve and (d) M–T curves of H40-1 and H60-1 treated under an rf power of 40 W and 60 W once; '×5' indicates that the curves have been re-scaled by a factor of 5 for a better view. All curves are for data at 300 K. The curve for Co_3O_4 in Fig. 1 is included as a reference for comparison. The inset of (a) shows the M–H curves of H20-1 and H20-4 measured at 10 K.

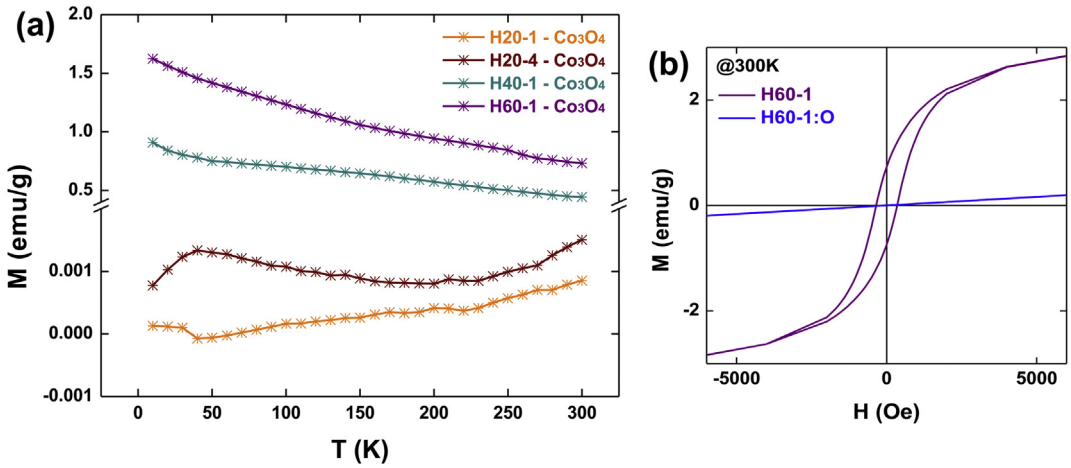

Fig. 4. (a) Difference in the M–T curves for H20-1, H20-4, H40-1, and H60-1, before and after hydrogen treatment of the Co_3O_4 samples. (b) Reaction of H60-1 to oxygen annealing. The Co metal precipitate is completely converted into Co_3O_4, and the ferromagnetism of the Co metal cluster disappears.

consistent with our conjecture. The small hysteresis loop with small squareness ratio also reflects a ferromagnetic feature of nano-sized magnetic precipitate due to its short-range ordering [10].

For a qualitative interpretation of the change in magnetization attributed to the creation of Co precipitates, we calculated differences of the temperature-dependent magnetization between each hydrogen-treated and untreated Co_3O_4. For a more precise estimation, we should consider the amount of Co_3O_4 transformed to Co phase, resulting in decrease in magnetization. However, it was not counted because such decrease is negligible compared to the increase accounted for by the ferromagnetism of the precipitates. Fig. 4(a) shows the differences in the M–T curves for H20-1, H20-4, H40-1, and H60-1 before and after hydrogen treatment. The size and quantity of Co cluster should increase with increasing rf power and number of hydrogen treatments. Specifically, the size of the Co clusters in H40-1 and H60-1 is expected to be above the nanoscale, approximately approaching the properties of the bulk. Billas et al. reported that the M–T curve for a Co metal cluster composed of 50–600 atoms has a positive slope that decreases with an increasing number of Co atoms [30]. As the positive tendency cannot be observed in the bulk, it is regarded as a unique characteristic of nano-sized Co clusters. Considering the fact that 1) the difference in magnetization before and after hydrogen treatment corresponds to an order of 10^{-4} emu/g, 2) the reported magnetization of the Co nano clusters [30] is on the order of 10^2 emu/g, and 3) total mass was counted for normalizing magnetization, the amount of Co clusters is estimated to be much less than 0.01% of the amount of Co_3O_4. The size of clusters was 50 nm at most. These results are consistent with the results obtained from the XRD measurements described above.

Gu et al. argue that the ferromagnetism of ZnCoO is caused by oxygen defects, based on their result that ferromagnetism disappeared after annealing process is carried out under oxygen [32]. However, as shown in Fig. 4(b), the ferromagnetic hysteresis loop of H60-1 disappears completely after annealing process under oxygen at 300 °C (H60-1:O) due to the oxidation of Co cluster. This result indicates that special care on the formation of Co nano cluster should be taken in investigating the magnetic contribution from defects. S. Deka et al. attributed the ferromagnetism of ZnCoO observed after hydrogen treatment to Co metal clusters formed by chemical reduction of Co–O bonding during high-temperature annealing [22]. These results suggest that the condition for post-hydrogen treatment should be optimized and that it is necessary to examine the existence of the Co_3O_4 phases prior to discussing the ferromagnetic origin in ZnCoO. Most importantly, we find that temperature-dependent magnetization measurement can be employed to detect nano-sized Co clusters below the detection limit of diffraction measurements.

4. Conclusion

Abnormal magnetic behavior attributed to nano size effects enables detection of nano-sized Co metal clusters below the XRD detection limit by measuring the temperature-dependent magnetization. The nano clusters were assumed to be ~50 nm in size and to make up less than 0.01% of the host material in quantity. Post hydrogen treatment to introduce crystalline defects or hydrogen impurities promotes creation of Co clusters if Co_3O_4 phase exists. The above results suggest that prior to the post treatment, it is necessary to confirm the absence of Co_3O_4. Moreover, this will provide a useful methodological approach to studying the ferromagnetic origin in Co-doped oxide semiconductors.

Acknowledgment

This research was supported by the Converging Research Center Program through the Ministry of Science, ICT and Future Planning, Korea (MSIP) (2013K000310), by the National Research Foundation of Korea (NRF) grant funded by the Korea government (MSIP) (No. 2011-0016525), and by the Financial Supporting Project of Long-term Overseas Dispatch of PNU's Tenure-track Faculty, 2012.

References

[1] H.-J. Lee, S.-Y. Jeong, C.R. Cho, C.H. Park, Appl. Phys. Lett. 81 (2002) 4020.
[2] Y. Yamada, K. Ueno, T. Fukunura, H.T. Yuan, H. Shimotani, Y. Iwasa, L. Gu, S. Tsukimoto, Y. Ikuhara, M. Kawasaki, Science 332 (2011) 1065.
[3] H.-J. Lee, C.H. Park, S.-Y. Jeong, K.-J. Yee, C.R. Cho, M.-H. Jung, D.J. Chadi, Appl. Phys. Lett. 88 (2006) 062504.
[4] H.B. de Carvalho, M.P. de Godoy, R.W.D. Paes, M. Mir, A.O. de Zevallos, F. Iikawa, M.J.S.P. Brasil, V.A. Chitta, W.B. Ferraz, M.A. Boselli, A.C.S. Sabioni, J. Appl. Phys. 108 (2010) 033914.
[5] T.C. Kaspar, T. Droubay, S.M. Heald, P. Nachimuthu, C.M. Wang, V. Shutthanandan, C.A. Johnson, D.R. Gamelin, S.A. Chambers, New J. Phys. 10 (2008) 055010.
[6] T. Dietl, T. Andrearczyk, A. Lipińska, M. Kiecana, M. Tay, Y. Wu, Phys. Rev. B 76 (2007) 155312.
[7] J.M.D. Coey, M. Venkatesan, C.B. Fitzgerald, Nat. Mater. 4 (2005) 173.
[8] G. Ciatto, A. Di Trolio, E. Fonda, P. Alippi, A.M. Testa, A.A. Bonapasta, Phys. Rev. Lett. 107 (2011) 127206.
[9] Y. Fukuma, F. Odawara, H. Asada, T. Koyanagi, Phys. Rev. B 78 (2008) 104417.

[10] S. Lee, Y.C. Cho, S.-J. Kim, C.R. Cho, S.-Y. Jeong, S.J. Kim, J.P. Kim, Y.N. Choi, J.M. Sur, Appl. Phys. Lett. 94 (2009) 212507.
[11] S.J. Kim, S. Lee, Y.C. Cho, Y.N. Choi, S. Park, I.K. Jeong, Y. Kuroiwa, C. Moriyoshi, S.-Y. Jeong, Phys. Rev. B 81 (2010) 212408.
[12] S.J. Kim, S.Y. Cha, J.Y. Kim, J.M. Shin, Y.C. Cho, S. Lee, W.-K. Kim, S.-Y. Jeong, Y.S. Yang, C.R. Cho, H.W. Cho, M.-H. Jung, B.-E. Jun, K.-Y. Kwon, Y. Kuroiwa, C. Moriyoshi, J. Phys. Chem. C 116 (2012) 12196.
[13] S. Lee, B.-S. Kim, S.-W. Seo, Y.C. Cho, S.K. Kim, J.P. Kim, I.-K. Jeong, C.R. Cho, C.U. Jung, H. Koinuma, S.-Y. Jeong, J. Appl. Phys. 111 (2012) 07C304.
[14] Y.C. Cho, S.-J. Kim, S. Lee, S.J. Kim, C.R. Cho, H.-H. Nahm, C.H. Park, I.K. Jeong, S. Park, T.E. Hong, S. Kuroda, S.-Y. Jeong, Appl. Phys. Lett. 95 (2009) 172514.
[15] J.M. Shin, H.S. Lee, S.Y. Cha, S. Lee, J.Y. Kim, N. Park, Y.C. Cho, S.J. Kim, S.-K. Kim, J.-S. Bae, S. Park, C.R. Cho, H. Koinuma, S.-Y. Jeong, Appl. Phys. Lett. 100 (2012) 172409.
[16] Y.C. Cho, S. Lee, H.H. Nahm, S.J. Kim, C.H. Park, S.Y. Lee, S.-K. Kim, C.R. Cho, H. Koinuma, S.-Y. Jeong, Appl. Phys. Lett. 100 (2012) 112403.
[17] L. Li, Y. Guo, X.Y. Cui, R. Zheng, K. Ohtani, C. Kong, A.V. Ceguerra, M.P. Moody, J.D. Ye, H.H. Tan, C. Jagadish, H. Liu, C. Stampfl, H. Ohno, S.P. Ringer, F. Matsukura, Phys. Rev. B 85 (2012) 174430.
[18] H.S. Hsu, J.C.A. Huang, Y.H. Huang, Y.F. Liao, M.Z. Lin, C.H. Lee, J.F. Lee, S.F. Chen, L.Y. Lai, C.P. Liu, Appl. Phys. Lett. 88 (2006) 242507.
[19] Z.H. Wang, D.Y. Geng, S. Guo, W.J. Hu, Z.D. Zhang, Appl. Phys. Lett. 92 (2008) 242505.
[20] H.S. Hsu, J.C.A. Huang, S.F. Chen, C.P. Liu, Appl. Phys. Lett. 90 (2007) 102506.
[21] R.K. Singhal, A. Samariya, Sudhish Kumar, Y.T. Xing, U.P. Deshpande, T. Shripathi, E. Baggio-Saitovitch, J. Magn. Magn. Mater. (2010) 2187.
[22] S. Deka, P.A. Joy, Appl. Phys. Lett. 89 (2006) 032508.
[23] H.-J. Lee, S.H. Choi, C.R. Cho, H.K. Kim, S.-Y. Jeong, Europhys. Lett. 72 (2005) 76.
[24] W.L. Roth, J. Phys. Chem. Solids 25 (1964) 1.
[25] P.J. van Zaag, Y. Ijiri, J.A. Borchers, L.F. Feiner, R.M. Wolf, J.M. Gaines, R.W. Erwin, M.A. Verheijen, Phys. Rev. Lett. 84 (2000) 6102.
[26] V. Papaefthimiou, T. Dintzer, V. Dupuis, F. Tournus, A. Tamion, A. Hillion, D. Teschner, M. Havecker, A. Knop-Gericke, R. Schlogl, S. Zafeiratos, ACS Nano 5 (2011) 2182.
[27] H. Boyen, G. Kästle, K. Zürn, T. Herzog, F. Weigl, P. Ziemann, O. Mayer, C. Jerome, M. Möller, J.P. Spatz, M.G. Garnier, P. Oelhafen, Adv. Funct. Mater. 13 (2003) 359.
[28] H.T. Zhu, J. Luo, J.K. Liang, G.H. Rao, J.B. Li, J.Y. Zhang, Z.M. Du, Phys. B 403 (2008) 3141.
[29] S.A. Makhlouf, J. Magn. Magn. Mater. 246 (2002) 184.
[30] I.M.L. Billas, A. Châtelain, W.A. de Heer, Science 265 (1994) 1682.
[31] Y. Xie, J.A. Blackman, J. Phys. Condens. Matter 16 (2004) 4373.
[32] H. Gu, W. Zhang, Y. Xu, M. Yan, Appl. Phys. Lett. 100 (2012) 202401.